

Effect of thermal loading on syntactic foam sandwich composite

Sunil Waddar¹  | Jeyaraj Pitchaimani²  | Mrityunjay Doddamani² 

¹Department of Mechanical Engineering, MVJ College of Engineering, Bangalore, India

²Department of Mechanical Engineering, National Institute of Technology Karnataka, Surathkal, India

Correspondence

Mrityunjay Doddamani, Department of Mechanical Engineering, National Institute of Technology Karnataka, Surathkal, India.
Email: mrdoddamani@nitk.edu.in

Abstract

An experimental investigation carried out on the deflection behavior of sandwich composites with a fly ash cenosphere/epoxy syntactic foam core and plain-woven sisal fiber fabric/epoxy skin subjected to nonuniform heating is presented. The influence of cenosphere volume fraction in the syntactic foam core, three different heating cases (*increase-decrease*, *decrease*, and *decrease-increase*), and cenospheres' surface treatment effect is analyzed. The temperature deflection is acquired with the help of a LabVIEW program. The critical buckling and snap-initiation temperatures are found from the temperature-deflection plots. It is observed that the sandwich beam undergoes snap-through buckling behavior due to viscoelastic forces associated with the syntactic foam core. The critical buckling temperature increases with the filler content, and the surface treatment enhances the buckling behavior marginally. Results also demonstrate that the sandwiching of the syntactic foam core between the natural fiber skin enhances critical buckling temperatures compared to the syntactic foam core.

KEYWORDS

fly ash cenosphere, natural fiber, sandwich beam, syntactic foam, thermal loading

1 | INTRODUCTION

Sandwich composites made with a syntactic foam core are gaining more popularity due to their high strength to weight ratio, light weight, high compression strength, and low moisture absorption.^[1,2] The rising environmental concern about carbon emissions because of man-made synthetic fibers can be effectively addressed through the use of naturally available resources for making sandwiches. Natural fiber reinforced in polymer matrix composites has found applications in marine and automobile industries due to its higher specific properties.^[3] Syntactic foams, being lightweight materials, provide better feasibility to design materials with varying volume fractions, change the wall thickness of particles, and use particles of different sizes.^[4-6] Glass microballoons and fly ash

cenospheres, which are spherical and possess excellent thermal insulation properties, are used as fillers in the polymeric matrix composites.^[7] As syntactic foams have good thermal stability and tailorable mechanical properties, they can be used in the cores of sandwich structures.^[8,9] Sandwich structures may experience an immense temperature difference, and due to in-plane loading caused by controlled thermal expansion, they may buckle.^[10] In addition, thermal buckling is one of the issues in the development of high-speed flight. In the design of sandwich composites for aerospace and marine applications, one crucial aspect is buckling. These structures may be subjected to aerodynamic heating, and the temperature rise may induce the buckling mode of failure.

Thermomechanical characterization of the syntactic foams is presented.^[7,11] Gu et al^[11] investigated the dynamic

mechanical properties of the surface-modified and as-received cenosphere/epoxy composites. They observed that the storage modulus was enhanced with an increase in filler content and with the surface modification of cenospheres. Mechanical properties of cenosphere/epoxy syntactic foams have been presented.^[5,6,12] Waddar et al^[13] investigated buckling and free vibration of cenosphere/epoxy syntactic foam core and sisal fiber/epoxy skin. Gupta et al^[14] investigated the flexural properties of sandwich composites with microballoons/epoxy syntactic foam core E-glass fiber/epoxy skins. They found that the core shear strength and skin-bending stress decrease with a radius ratio of microballoons. George et al^[15] investigated the buckling behavior of aluminum beams subjected to nonuniform thermal loads numerically and experimentally. Bhagat and Jeyaraj^[16] investigated the buckling behavior of aluminum shells exposed to nonuniform temperature profiles. Recently, Waddar et al^[17] investigated the snap-through buckling behavior of the cenosphere/epoxy syntactic foam composites and observed that the beams stay in the first buckled position for a longer duration with an increase in filler content. Nonetheless, research articles on the buckling behavior of sandwich composites with syntactic foam core and natural fiber skins are yet to be reported.

Buckling under in-plane compression of sandwich composites made of Klegcell foam core and S2-glass/vinyl ester face sheets is studied by Mahfuz et al.^[18] Their results demonstrate increased buckling loads with the density of the core material and show that high-density cores arrest the delamination between core and skin and core shearing phenomena during buckling. Pradeep et al^[19] analyzed vibration and thermal buckling characteristics of soundcoat-DYAD609 viscoelastic core and graphite/epoxy skin sandwich beam and plate using the finite element method. Lan et al^[20] numerically investigated a three-layered bimodular sandwich beam (thick skins and moderately stiff cores) subjected to uniform and nonuniform thermal loads. Liu et al^[21] investigated the buckling behavior of the E-glass/vinyl ester laminate column subjected to combined axial compressive and uniform thermal loads. They observed that the structure bends away from the heating source at lower temperatures and toward the heating source at higher temperatures due to thermal moment. Yuan et al^[22] experimentally investigated the thermal buckling behavior of sandwich structures with a pyramidal truss core. Shiau and Kuo^[23] numerically investigated the post-buckling behavior of graphite-epoxy laminated face sheets and aluminum honeycomb core sandwich panels subjected to uniform thermal load. Mirzaei and Kiani^[24] analytically examined snap-through buckling of sandwich beams made of functionally graded carbon nanotube (CNT) skin and homogeneous/isotropic core. Sandwich beams with CNT face sheet and isotropic core subjected to thermal load is analyzed

using an analytical method by Kiani.^[25] The thermal buckling behavior of sandwich plates with laminated face sheets and a honeycomb core was investigated numerically by Shiau and Kuo.^[26] They reported that the buckling mode and buckling temperature are dependent on the fiber orientation and aspect ratio of the plate. Chao and Lin^[27] numerically investigated static and dynamic snap-through buckling of sandwich spherical caps. They observed that the dynamic buckling loads are much lower than the static buckling loads. Bouazza et al^[28] analytically investigated the thermal buckling behavior of jute fiber reinforced in epoxy laminate beams using higher-order shear deformation theory. The results were found to be in good agreement with other published literature.

From the existing literature, it is clear that cenosphere/epoxy syntactic foam core sandwich with natural fiber skin has not been investigated for its behavior under nonuniform heating conditions. However, it is crucial to study this behavior for the better design of the syntactic foam core sandwich composites. In the present experimental investigation, sandwich beams with sisal fabric/epoxy skins and cenosphere/epoxy syntactic foams through varying volume fractions of untreated and treated cenospheres (0%, 20%, 40%, and 60%) in the epoxy matrix are prepared. Temperature is varied in a range of 26°C to 60°C for three different heating conditions (case i: *increase-decrease*, case ii: *decrease*, and case iii: *decrease-increase*). The effect of temperature variation and filler content on the thermal buckling behavior of sandwich composites is presented in this work. The deflection behavior of sandwich beams subjected to three different heating conditions is studied, and critical buckling temperature is found from the temperature rise-deflection curves.

2 | MATERIALS AND METHODS

2.1 | Constituents materials

Diglycidyl ether of bisphenol-A epoxy resin (LAPOX L-12) and room-temperature curing agent Polyamine (K-6) hardener, both procured from Atul Ltd., Gujarat, India, are used as a matrix material to prepare the skin and cores of sandwich composites. Sisal plain-woven fabric acquired from Jolly Enterprises, Kolkata, West Bengal, India, is used as skin in a sandwich. Cenospheres (CIL 150 grade) purchased from Cenosphere India Pvt Ltd, Kolkata, West Bengal, India are used as fillers in an epoxy matrix. The cenospheres reinforced in the epoxy matrix are used as a core material in the sandwich. Cenospheres are produced as byproducts of thermal power plants, which are available abundantly and are spherical and hollow. The major

constituents of cenospheres are alumina, silica, and iron oxide. Untreated (as received) and 3-Amino Propyl tri ethoxy silane-treated cenospheres in epoxy as syntactic foam cores are further utilized in the sandwich. The procedure for surface treatment and silane coating confirmatory tests are outlined.^[29]

2.2 | Syntactic foam preparation

Syntactic foam cores are prepared with untreated (as received) and treated cenospheres with changing cenosphere volume fraction of 0%, 20%, 40% and 60% in an epoxy matrix. A known quantity of epoxy resin is taken into a beaker, and requisite cenospheres are added and stirred gently until a homogenous mixture is obtained. Subsequently, the K6 hardener (10 wt%) is added to the mixture and stirred gently. After the initiation of the polymerization of the homogenous mixture, the slurry is poured into the mold. To remove the cast slabs easily, the mold is coated with a silicone-releasing agent. The cast slabs are removed from the mold after curing (24 h) at room temperature. The syntactic foam slabs are then reduced to a thickness of 2.5 mm using a belt (120 grit size) polishing machine and later cleaned using acetone.

2.3 | Sandwich preparation

The hand lay-up process is used to prepare syntactic foam sandwich composites with sisal fabric/epoxy skins. A sequence of operations used in making sandwich

composites is presented in Figure 1. The mold cavity has a total depth of 4 mm, which will be imparted to the sandwich. The single layer of sisal fabric is drenched in the epoxy matrix and placed first on the bottom plate of the empty mold (Figure 1A,B). Subsequently, the earlier prepared foam core is placed on the wet sisal fabric (Figure 1C), which forms the bottom skin. The top skin, in the form of drenched sisal fabric, is laid immediately on the top of the foam core (Figure 1D). Finally, the mold is closed from the top with the upper plate and is rigidly clamped (Figure 1E). The sandwich castings are further cured at room temperature for 24 h. Subsequently, sandwich samples are removed from the mold (Figure 1F,G) and trimmed to $370 \times 12.5 \times 4$ mm^[17] (Figure 1H,I) using a diamond saw cutter. The mechanical interlocking takes place between skins and a relatively rough foam core surface under clamping forces. All the sandwiches prepared are coded as per nomenclature SEXXY, where letter 'S' represent sisal/epoxy facing, alphabet 'E' represents neat epoxy resin, 'XX' denote cenosphere volume fraction, and 'Y' represents untreated (U) or treated (T) syntactic foam core.

2.4 | Density test

Experimental densities of the foam cores and sandwiches are carried out using ASTM D792-13. Five samples of each composition are tested, and the average values with standard deviations are reported (Tables 1 and 2). The theoretical density of syntactic foam cores are computed using the rule of mixtures as,

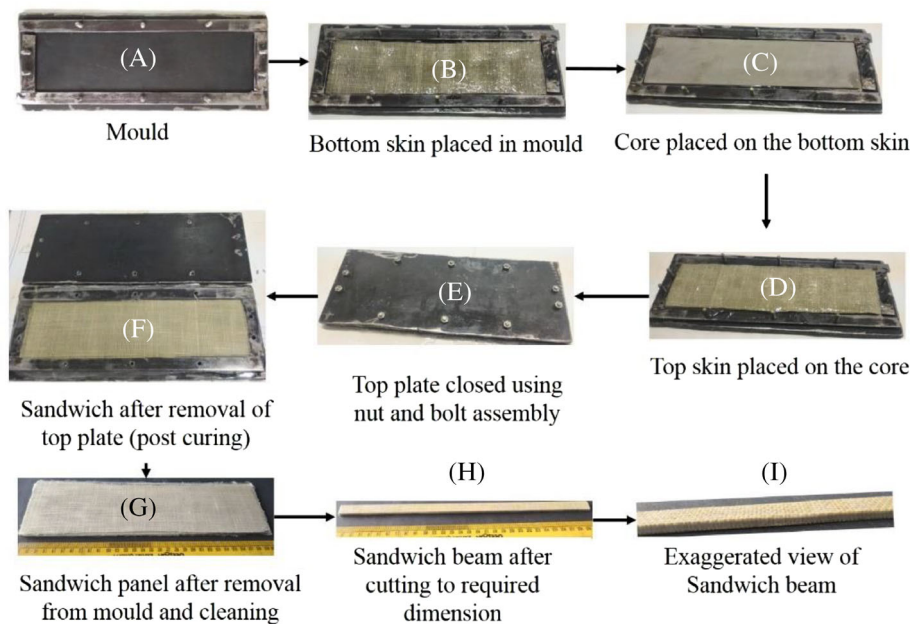


FIGURE 1 Sequence of sandwich construction [Color figure can be viewed at wileyonlinelibrary.com]

TABLE 1 Densities of neat epoxy and their foams^[17,29]

Material type	Theoretical density (kg/m ³)	Experimental density (kg/m ³)	Matrix void content (%)	Weight-saving potential
E0	1189.54	1189.54 ± 0.04	—	—
E20U	1135.63	1113.01 ± 3.56	1.99	6.43
E40U	1081.72	1057.74 ± 6.48	2.22	11.08
E40U	1027.82	1001.49 ± 9.54	2.56	15.81
E20T	1151.63	1122.05 ± 3.69	2.57	5.67
E40T	1113.72	1062.10 ± 3.70	4.63	10.71
E60T	1075.82	1015.75 ± 3.71	5.58	14.61

TABLE 2 Experimental densities of sandwich composites

Material type	Theoretical density (kg/m ³)	Experimental density (kg/m ³)	Matrix void content (%)
SE0	1236.93	1225.80 ± 1.09	0.91
SE20U	1203.24	1177.97 ± 2.99	2.10
SE40U	1169.54	1142.64 ± 5.68	2.30
SE60U	1135.86	1105.19 ± 8.24	2.71
SE20T	1213.24	1181.69 ± 3.88	2.61
SE40T	1188.92	1148.73 ± 4.28	3.38
SE60T	1165.86	1112.89 ± 7.17	4.54

$$\rho^{th} = \rho_c V_c + \rho_m V_m \quad (1)$$

where ρ and V represent density and volume fraction, respectively, and suffices m and c represent the matrix and filler, respectively. The theoretical density of syntactic foam sandwich composites with natural fiber/epoxy skin is estimated using Equation 2.

$$\rho^{th} = (\rho_c V_c + \rho_m V_m)_{core} + (\rho_f V_f + \rho_m V_m)_{skin} \quad (2)$$

The suffix f in Equation 2 represents fiber. The air entrapped during the mixing of cenospheres in a matrix and during the hand lay-up process is called voids. Void content (ϕ_v) in the syntactic foam and sandwich composite is computed by accounting for the relative difference between the theoretical and experimentally measured density as,

$$\phi_v = \frac{\rho^{th} - \rho^{exp}}{\rho^{th}} \quad (3)$$

2.5 | Thermal buckling test

The in-house developed thermal buckling test setup, as presented in Figure 2, is used for measuring thermal load

and deflections.^[15] Single-tube short-wave infrared (IR) heating lamps (230 V/1000 W) are used to heat the sandwich beams. These IR lamps are placed at different positions lengthwise (Figure 3) to accomplish different nonuniform temperature profiles and are placed 30 mm away from the lateral surface of the beam. Both ends of the sandwich beams are rigidly clamped using a mild steel frame resembling a clamped-clamped condition.

Furthermore, specimens are exposed to thermal load through the radiation heat transfer of the IR heating source. Lateral deflection of the beams is measured using a linear variable differential transducer (LVDT) of Honeywell (Model: MVL7 LVDT) with a stroke length of ±25.4 mm that operates in the range of −50°C to +125°C. K-type thermocouples with a sensitivity of 41 μV/°C are used to measure temperatures at dissimilar positions lengthwise and are recorded in personal computers through the data acquisition system (DAQ). A relay unit is used to control the ON/OFF state of the IR heater based on the thermocouple output using the LabVIEW program, which in turn plots temperature rise-deflection curves.

The IR heating lamps are used to heat the sandwich samples through the radiation mode of heat transfer. These IR lamps are operated till the desired temperature is reached, which is set in the LABVIEW program initially. The ON/OFF switch of the IR heating lamps is based on the desired input, which is controlled by NI9481 DAQ. This NI9481 DAQ has four-channels and is of solo pole and solo throw digital output module, which presents the digital ON/OFF signal generated by the LABVIEW program triggering the voltage regulator. Due to the application of thermal load and constrained boundary conditions, thermal stresses develop, resulting in out-of-plane deflections. This deflection is measured using LVDT (NI9215 DAQ) and temperature using K-type thermocouples (NI9211 DAQ). The root mean square values of temperature-deflection data are stored using a shift register in a proper array through the LABVIEW program.

FIGURE 2 A, Actual test set-up used.
B, Test specimen clamped in mild steel frame
[Color figure can be viewed at
wileyonlinelibrary.com]

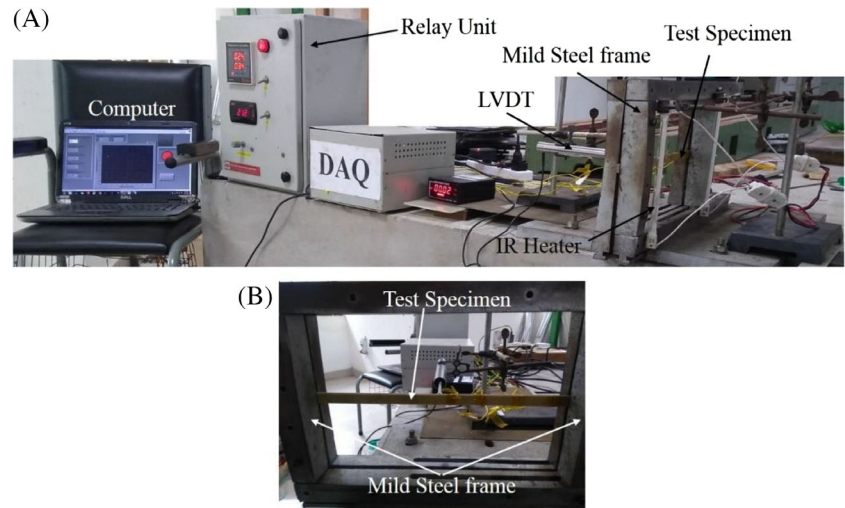
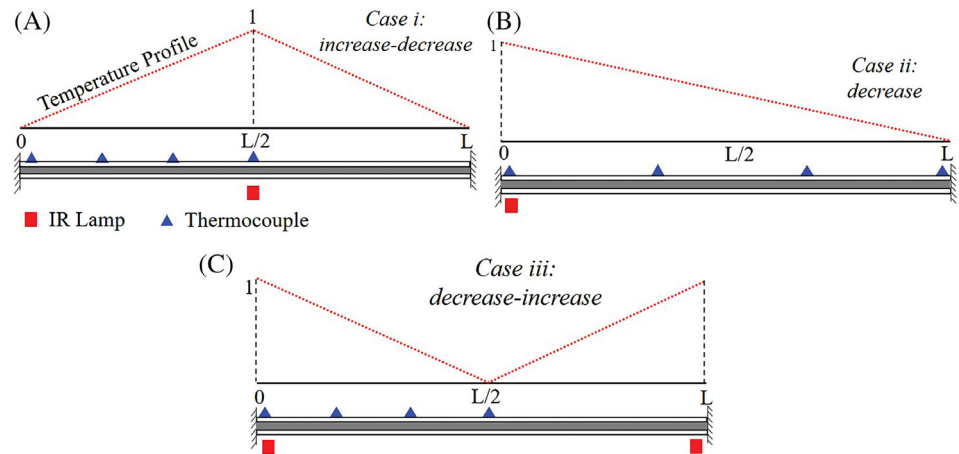


FIGURE 3 Schematic representation of nonuniform thermal heating cases [Color figure can be viewed at
wileyonlinelibrary.com]



Furthermore, these values are plotted in Microsoft Excel sheets using the write command. Once the experiments are completed, modified Budiansky criteria are used to find buckling temperatures.^[30] The reader is referred to George et al^[15] for more details on the thermal buckling setup.

Three different types of nonuniform temperature profiles (case i, case ii, and case iii) are considered by placing the IR heating lamps in different locations (Figure 3). In case i: *increase-decrease* heating, the IR lamp is placed at the beam center (Figure 3A), and therefore, highest temperature is at the mid-portion and the least at the ends. In case ii, the *decrease* heating condition (Figure 3B), the IR heating lamp is fixed at one end of the beam, resulting in higher temperatures at one end and the lowest temperature at the other end. Figure 3C represents the case iii (*decrease-increase*) condition, where IR lamps are located at both ends of the beam. These three cases represent a broad spectrum of nonuniform thermal loading, which may resemble practical in-service conditions.

3 | RESULTS AND DISCUSSION

3.1 | Microstructure and material processing

Figure 4 shows the micrographs of untreated and silane-treated cenospheres. From Figure 4, one can observe that cenospheres are spherical and have numerous defects on the surface. Such defects lead to deviations of experimental results from theoretical ones. The particle size analysis and Fourier (FTIR) results are discussed.^[29] The average thickness of the dry skin is computed to be 0.723 mm, and the measured density of sisal yarn is found to be 1262.86 ± 46.21 kg/m³. The homogenous mixing of cenospheres with no agglomeration is evident from Figure 5B,C. Yarns of the sisal fabrics are seen to completely cover the epoxy matrix by signifying proper wetting of fibers by epoxy resin (Figure 5B,C) during processing. Proper bonding between sisal fiber facing and syntactic foam is evident from Figure 5B,C. Density and void content present in the syntactic foam and their

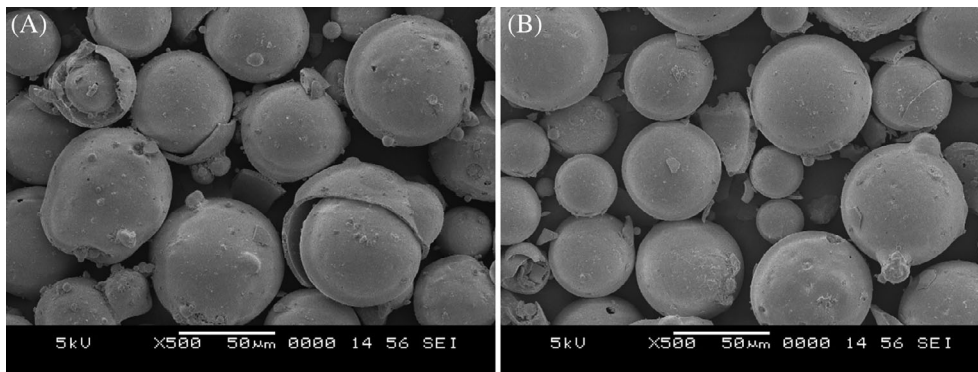


FIGURE 4 Micrographs of (A) untreated and (B) treated cenospheres

sandwiches need to be looked into to assess the quality of prepared samples.

3.2 | Density of syntactic foams and their sandwiches

The quality and properties of sandwich composites made with syntactic foams cores are dependent on the amount of survived hollow particles and void content. The presence of air entrapment during the mixing of cenospheres in epoxy resin and hand lay-up process during sandwich construction is considered void content. Tables 1 and 2 present densities and void content of syntactic foams and their sandwiches, respectively. Theoretical densities are calculated using Equations 1 and 2, which are noted to be higher compared to experimental values (Tables 1 and 2). Void content in prepared sandwiches is less than 4.5%, indicating good-quality samples. Experimental density values, compared to theoretical ones, are found to be lower and are attributed to air entrapment during the mechanical mixing of constituent materials in foam cores. Wetting of the fabric in epoxy results in an additional air entrapment in facings. The weight-saving potential (Table 1) in the range of 5.67% to 15.81% is attained in syntactic foams. Exploring these lightweight syntactic foams in sandwich composites makes them suitable for marine and aerospace applications owing to higher specific mechanical and thermal properties. It is worth investigating when such sandwiches are subjected to thermal buckling.

3.3 | Buckling under nonuniform heating

The sandwich beams are subjected to three different heating conditions, as shown in Figure 2. The highest temperature of a temperature profile and transverse deflections of the beam are recorded using a

thermocouple and LVDT, and results are further used to plot temperature rise-deflection response. As the beams were expected to deflect in the first bending mode and at the middle portion along the length, deflections are measured at the midpoint of the beam. For all the tested samples, it is observed that initial deflections take place away from the heating source and later toward the heating source at higher temperatures. The deflection away from the heating source is considered to be positive and toward the heating source is considered negative. To understand the deflection trend of the syntactic foam sandwich beam, the temperature rise-deflection plot associated with SE40U subjected to the case i (*increase-decrease*) heating condition is presented in Figure 6A. As the temperature increases, prepared samples undergo the following four trends in general.

Region I: When the beam is exposed to heat, it is not experiencing any significant deflection amid significant temperature rise. A portion of the deflection curve *a-b* (Figure 6A) indicates this clearly. This also suggests that the temperature rise till point *b* is unable to develop a sufficient amount of compressive stress to cause any significant amount of out-of-plane deflection. However, the behavior of syntactic foam is different as seen in Figure 6B. A detailed explanation for the deflection behavior of the syntactic foam beam under similar heating conditions is presented.^[17] Sandwiching of syntactic foam between the natural fiber/epoxy laminate facings controls the out-of-plane deflection. This is attributed to structural stiffness enhancement due to the sandwich effect.

Region II: With a further increase in temperature beyond point *b*, the out-of-plane deflection increases drastically even with a small rise in temperature (*b-c*). It is observed that the deflection behavior between points *b* and *c* is linear, and the sandwich beam deflects away from the heating source. The reason for this drastic increase in deflection in this region can be attributed to the compressive stresses developed and thermal moments therein due to the heating effect.^[21] The portion of curve

FIGURE 5 A, Schematic representation of sandwich. B, Micrographs of freeze-fractured top skin. C, Bottom skin interface of representative SE40T sample [Color figure can be viewed at wileyonlinelibrary.com]

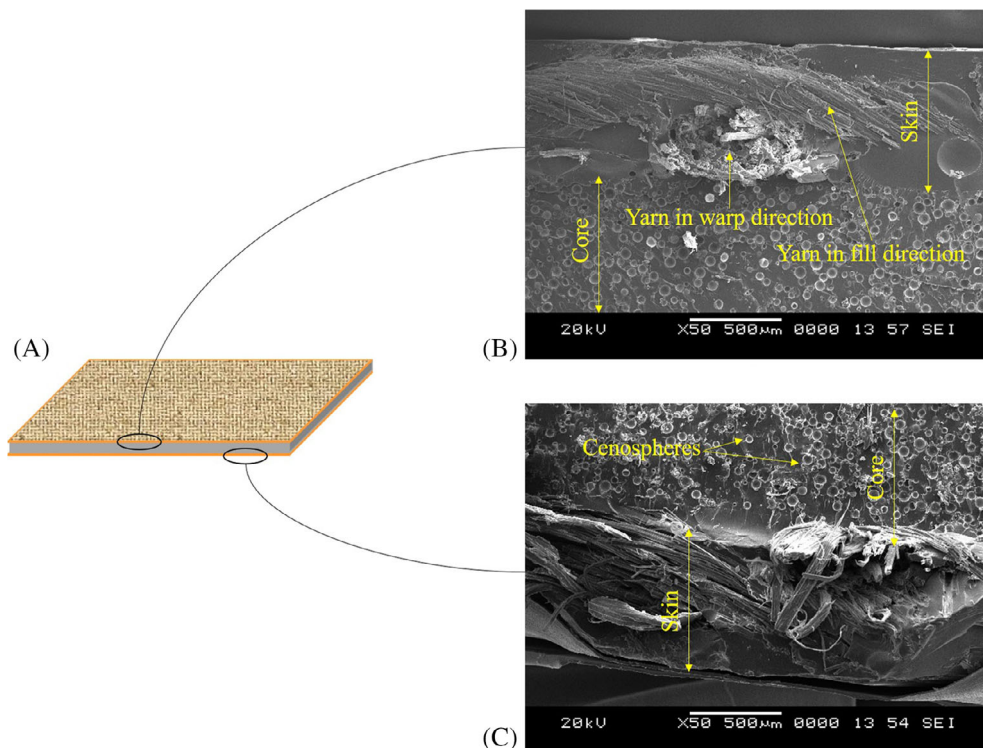
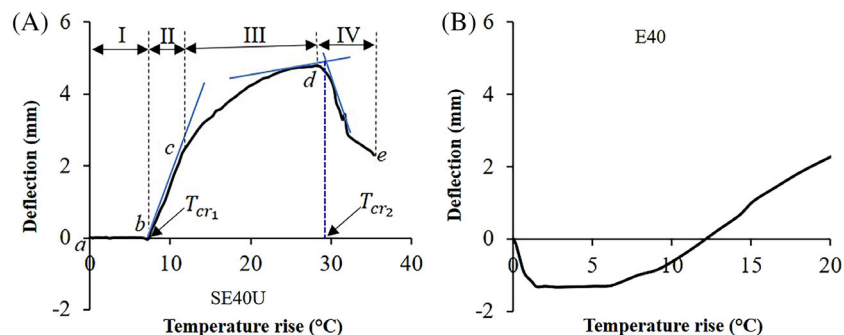


FIGURE 6 A, Determination of critical buckling temperatures from temperature-deflection curve. B, Temperature deflection of E40 sample [Color figure can be viewed at wileyonlinelibrary.com]



from a - c shows typical load-deflection behavior of a beam under a compressive load, and the first bifurcation point is observed to be at b (T_{cr1}).

Region III: With further increase in temperature rise beyond point c , the beam continues to deflect in the same direction till point d . However, the rate of increase in deflection concerning temperature rise is not as rapid as that observed in Region II. This change in rate of deflection may be due to the energy storage of the sandwich beam developed during temperature rise.^[17]

Region IV: With further increase in the temperature beyond point d , the beam deflects toward the heating source. Temperature rise corresponding to point d is considered the snap-initiation temperature (T_{cr2}).

Figure 6A represents the method used to estimate T_{cr1} and T_{cr2} . For all the tested samples, it is observed that deflections take place away from the heating source

initially at lower temperatures and toward the heating source at higher temperatures. The trend observed for cenosphere/epoxy syntactic foams and their sandwiches with sisal/epoxy skins is entirely different, as evident from Figure 6A,B, respectively. Syntactic foams undergo deflection initially for a small temperature rise ($<2^{\circ}\text{C}$) and retain the first buckled shape for a longer duration. Snap-through phenomena take place due to the viscoelastic forces developed in the syntactic foam beam. However, in sandwiches, the beam remained in its positions for the initial temperature rise and later underwent deflection. The sandwich beams with a syntactic foam core exhibited snap-through phenomena at very high temperatures compared to that of syntactic foams.

Buckling behavior of sandwich composites with neat epoxy core and a syntactic foam core under different heating conditions is shown in Figure 7. It is observed

that, with an increase in cenosphere content, the first critical buckling temperature increases, and the deflection of the beams decreases. This can be attributed to the enhanced stiffness of the composite due to the addition of stiff cenospheres to the epoxy matrix in addition to the

sandwich effect. The time duration of the beam retaining the first buckling mode shape increases with filler content. With an increase in temperature, a significant amount of viscoelastic forces develops in the sandwich beams. This time-dependent phenomenon keeps the

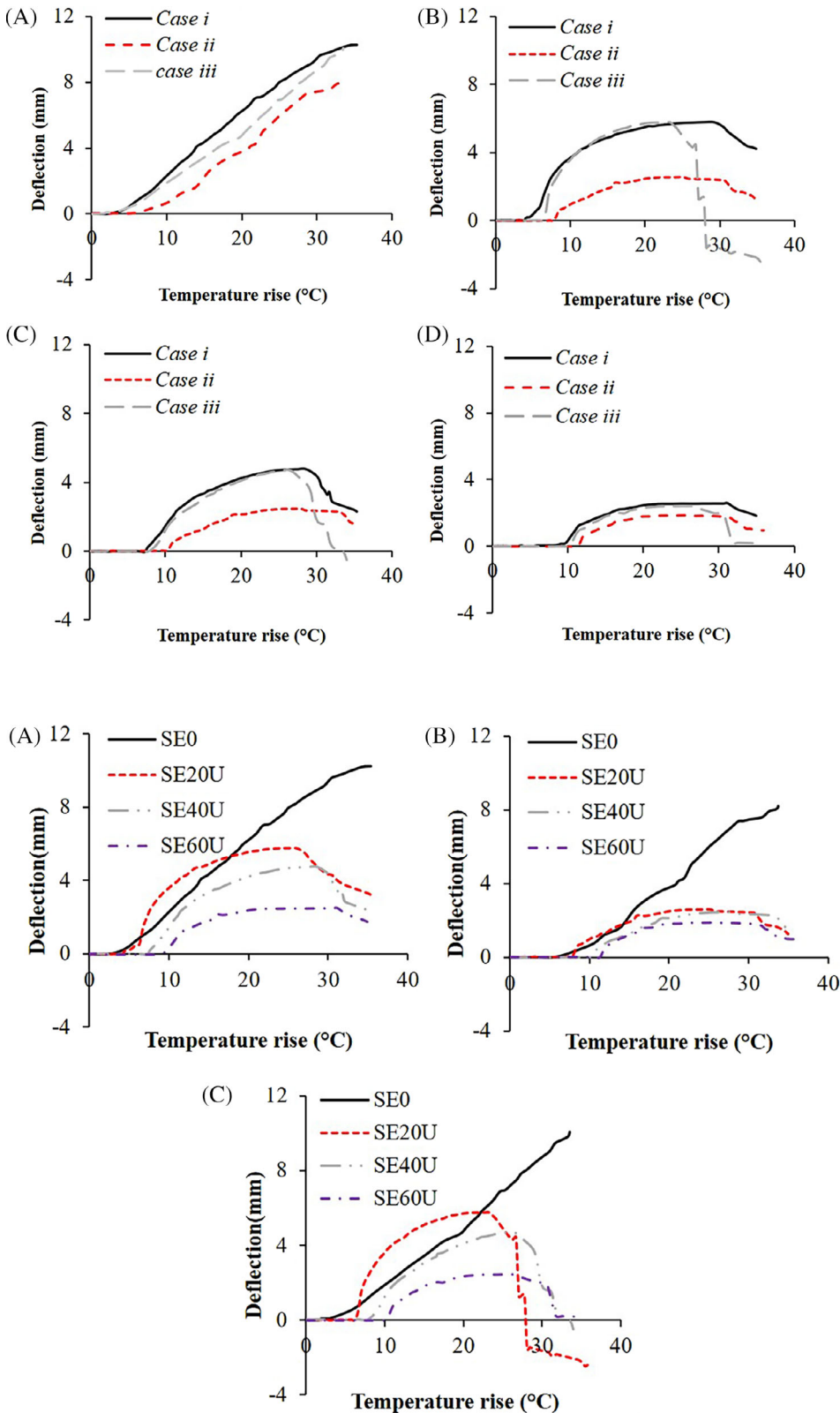
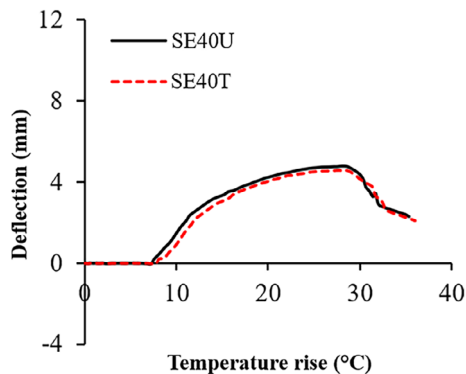


FIGURE 7 Effect of nonuniform heating of (A) SE0, (B) SE20U, (C) SE40U, and (D) SE60U sandwich composites [Color figure can be viewed at wileyonlinelibrary.com]

FIGURE 8 Effect of filler content on (A) increase-decrease, (B) decrease, and (C) decrease-increase heating conditions [Color figure can be viewed at wileyonlinelibrary.com]

TABLE 3 Thermal buckling temperatures of the sandwich composites subjected to nonuniform thermal loads

Sample coding	Case i: <i>increase-decrease</i>		Case ii: <i>decrease</i>		Case iii: <i>decrease-increase</i>	
	T_{cr_1} (°C)	T_{cr_2} (°C)	T_{cr_1} (°C)	T_{cr_2} (°C)	T_{cr_1} (°C)	T_{cr_2} (°C)
SE0	3.82 ± 0.46	—	6.25 ± 0.69	—	4.28 ± 0.82	—
SE20U	4.18 ± 0.58	29.15 ± 1.53	6.28 ± 0.76	30.5 ± 1.89	7.80 ± 0.29	23.25 ± 1.95
SE40U	7.25 ± 1.02	30.50 ± 1.68	10.25 ± 0.98	33.56 ± 1.28	8.16 ± 0.50	28.15 ± 1.30
SE60U	8.75 ± 1.09	30.25 ± 1.59	11.30 ± 1.08	32.60 ± 2.41	10.12 ± 1.21	29.15 ± 2.05
SE20T	4.85 ± 0.41	28.15 ± 1.41	8.2 ± 0.64	31.25 ± 1.54	7.05 ± 0.62	25.75 ± 2.01
SE40T	8.15 ± 0.40	31.78 ± 1.13	11.08 ± 0.84	34.68 ± 1.22	9.17 ± 1.21	29.15 ± 2.03
SE60T	9.58 ± 0.69	32.05 ± 2.49	12.86 ± 2.67	33.66 ± 2.41	11.06 ± 1.20	29.98 ± 2.92

**FIGURE 9** Effect of surface modification on thermal buckling behavior of representative sandwich sample [Color figure can be viewed at wileyonlinelibrary.com]

beam in the same buckled shape for a particular period with temperature rise. With further increases in temperature and cenosphere content, compressive stresses and viscoelastic forces creep in, and the buckled beam deforms back toward the original position. This trend is observed for all the sandwich composites subjected to all the three different heating conditions.

Figure 8 represents temperature-deflection curves for sandwich beams with neat resin and syntactic foam cores subjected to various thermal loading conditions (Figure 2). In practical cases where the nonuniform heating of structures takes place, the critical buckling temperatures and deflection behavior are prominently dependent on the location of the heating source and area of structural beam member exposed to the highest temperature for the particular temperature profile. From Figure 8, it is clear that the deflection trend observed for all the heating conditions is similar until the snap-initiation position of the beams. In case iii: *decrease-increase* (Figure 3C) heating case, snap-through phenomena are quicker than the other two heating conditions. This phenomenon may be due to more viscoelastic forces developing due to the higher intensity of

heating. *Increase-decrease* (Figure 3A) heating reported lower critical buckling temperatures and snap-through initiation temperature (Table 3), which can be attributed to the location of the heating source. In the case of *increase-decrease* heating, the source is located at the center of the beam where the sandwich beam offers less stiffness. Hence, the critical buckling temperatures are lower compared to other heating cases. In case ii: *decrease* (Figure 3B) condition, the sandwich beam is exposed to a higher temperature at one of its constrained ends. The rate of reduction in structural stiffness is lower compared to other heating conditions, resulting in higher critical buckling temperature and higher snap-initiation temperatures. In *decrease-increase* heating (Figure 3C), the intensity of heat is more at both the ends, and the rate of reduction in structural stiffness is not higher compared to the *increase-decrease* heating cases. Therefore, deflections are lower than the *increase-decrease* case.

The surface-modified cenosphere/epoxy syntactic foam sandwich composites show slight enhancement in the critical buckling temperatures and snap-initiation temperatures (Figure 9 and Table 3). The critical buckling temperature values are also found to be within the SD values of the untreated cenosphere/epoxy syntactic foam sandwich composites. Surface modification of the cenospheres enhances proper interfacial bonding between the constituents, increasing sandwich core material stiffness. A test of progress images of the sample is represented in Figure 10. The effect of stiffness enhancement of the core due to surface modification is not reflected in the improvement of critical buckling temperatures when subjected to the three different heating conditions (Figure 3). Sandwich beams with untreated and treated cenosphere/epoxy syntactic foam with woven fabric sisal skin exhibited higher critical buckling temperatures, and further temperature rises undergo snap-through buckling when subjected to the nonuniform thermal loads. These materials can be used for structural

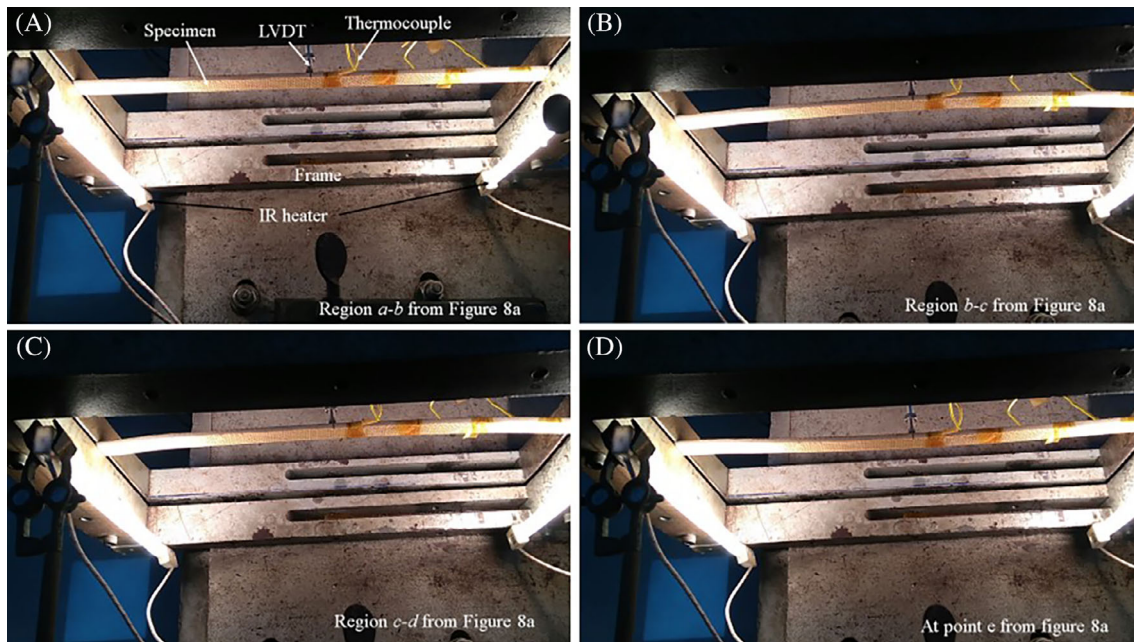


FIGURE 10 Test of progress images of the representative sample under decrease-increase heating condition [Color figure can be viewed at wileyonlinelibrary.com]

applications as a lightweight material system in marine, automobile, and aerospace sectors.

4 | CONCLUSIONS

Sandwich composites with cenosphere/epoxy syntactic foam composite cores and woven fabric/epoxy sisal skins are prepared and tested under nonuniform heating conditions for their deflection behavior. Micrographs of the sandwich sample at the skin-core interface indicated good bonding with very low void content. All the tested samples subjected to thermal load undergo deflection away from the heating sources at lower temperatures and toward the heating source at the higher temperatures. The critical buckling temperature shows an increasing trend with filler content. Surface-modified cenosphere/epoxy sandwich composites do not show a significant increase in buckling temperatures. Nevertheless, lower deflections are observed due to the increased stiffness of the foams.

ACKNOWLEDGEMENT

The authors thank the Mechanical Departments of NIT-K and MVJCE for providing facilities and support.

ORCID

Sunil Waddar  <https://orcid.org/0000-0002-0331-9637>

Jeyaraj Pitchaimani  <https://orcid.org/0000-0002-8456-8052>

Mrityunjay Doddamani  <https://orcid.org/0000-0002-5537-9404>

REFERENCES

- [1] D. D. Luong, L. Ansuini, N. Gupta, Dynamic Response of Syntactic Foams and Sandwich Composites: Blast and High Strain Rate Loading. in *Blast Mitigation Strategies in Marine Composite and Sandwich Structures* (Eds: S. Gopalakrishnan, Y. Rajapakse), Springer Singapore, Singapore **2018**, p. 171.
- [2] M. L. Jayavardhan, M. Doddamani, *Compos Part B Eng* **2018**, *149*, 165.
- [3] C. Fragassa, Marine Applications of Natural Fibre-Reinforced Composites: A Manufacturing Case Study. in *Advances in Applications of Industrial Biomaterials* (Eds: E. Pellicer, D. Nikolic, J. Sort, et al.), Springer International Publishing, Cham **2017**, p. 21.
- [4] N. Gupta, S. E. Zeltmann, V. C. Shunmugasamy, D. Pinisetty, *JOM* **2014**, *66*, 245.
- [5] K. Shahapurkar, V. B. Chavan, M. Doddamani, G. C. M. Kumar, *Wear* **2018**, *414-415*, 327.
- [6] C. D. Garcia, K. Shahapurkar, M. Doddamani, G. C. M. Kumar, P. Prabhakar, *Compos Part B Eng* **2018**, *151*, 265.
- [7] M. Labella, S. E. Zeltmann, V. C. Shunmugasamy, N. Gupta, P. K. Rohatgi, *Fuel* **2014**, *121*, 240.
- [8] N. Gupta, S. E. Zeltmann, D. D. Luong, M. Doddamani, 7—Core Materials for Marine Sandwich Structures. in *Marine Composites* (Eds: R. Pemberton, J. Summerscales, J. Graham-Jones), Woodhead Publishing, Duxford, UK **2019**, p. 187.
- [9] M. R. Doddamani, S. M. Kulkarni, *Polym Compos* **2011**, *32*, 1541.
- [10] J. M. Quintana, T. M. Mower, *Mater Design* **2017**, *135*, 411.
- [11] J. Gu, G. Wu, Q. Zhang, *Mater Sci Eng A* **2007**, *452-453*, 614.

- [12] K. Shahapurkar, C. D. Garcia, M. Doddamani, G. C. Mohan Kumar, P. Prabhakar, *Compos Part B Eng* **2018**, *135*, 253.
- [13] S. Waddar, J. Pitchaimani, M. Doddamani, E. Barbero, *Compos Part B Eng* **2019**, *175*, 107133.
- [14] N. Gupta, E. Woldesenbet, *J Compos Mater* **2005**, *39*, 2197.
- [15] N. George, P. Jeyaraj, S. M. Murigendrappa, *Thin-Walled Struct* **2016**, *108*, 245.
- [16] V. Bhagat, P. Jeyaraj, *Int J Non-Linear Mech* **2018**, *99*, 247.
- [17] S. Waddar, J. Pitchaimani, M. Doddamani, *Thin-Walled Struct* **2018**, *131*, 417.
- [18] H. Mahfuz, S. Islam, M. Saha, L. Carlsson, S. Jeelani, *Appl Compos Mater* **2005**, *12*, 73.
- [19] V. Pradeep, N. Ganesan, K. Bhaskar, *Compos Struct* **2007**, *81*, 60.
- [20] T. Lan, P. D. Lin, L. W. Chen, *Compos Struct* **1993**, *25*, 345.
- [21] L. Liu, G. A. Kardomateas, V. Birman, J. W. Holmes, G. J. Simitzes, *Compos Part A Appl Sci Manuf* **2006**, *37*, 972.
- [22] W. Yuan, H. Song, X. Wang, C. Huang, *AIAA J* **2014**, *53*, 948.
- [23] L.-C. Shiau, S.-Y. Kuo, *J Eng Mech* **2004**, *130*, 1160.
- [24] M. Mirzaei, Y. Kiani, *Compos Struct* **2015**, *134*, 1004.
- [25] Y. Kiani, *J Thermal Stress* **2016**, *39*, 1098.
- [26] L.-C. Shiau, S.-Y. Kuo, *Mech Based Design Struct Mach* **2004**, *32*, 57.
- [27] C. C. Chao, I. S. Lin, *Compos Struct* **1990**, *14*, 281.
- [28] M. Bouazza, N. Benseddiq, A. Zenkour, *J Thermal Stress* **2018**, *41*, 1.
- [29] S. Waddar, P. Jeyaraj, M. Doddamani, *J Compos Mater* **2018**, *52*, 2621.
- [30] M. Shariyat, *Thin-Walled Struct* **2007**, *45*, 439.

How to cite this article: Waddar S, Pitchaimani J, Doddamani M. Effect of thermal loading on syntactic foam sandwich composite. *Polymer Composites*. 2020;1–11. <https://doi.org/10.1002/pc.25496>